
Continuous Perception Benchmark

Anonymous Author(s)

Affiliation

Address

email

Abstract

1 Humans continuously perceive and process visual signals. However, current video
2 models typically either sample key frames sparsely or divide videos into chunks
3 and densely sample within each chunk. This approach stems from the fact that most
4 existing video benchmarks can be addressed by analyzing key frames or aggregating
5 information from separate chunks. We anticipate that the next generation of vision
6 models will emulate human perception by processing visual input continuously
7 and holistically. To facilitate the development of such models, we propose the
8 Continuous Perception Benchmark, a video question answering task that cannot
9 be solved by focusing solely on a few frames or by captioning small chunks and
10 then summarizing using language models. Extensive experiments demonstrate that
11 existing vision models, whether commercial or open-source, struggle with these
12 tasks, indicating the need for new technical advancements in this direction.

13 1 Introduction

14 Video understanding is a foundational task in computer vision that has been extensively studied for
15 decades. Over the years, a variety of methods have been developed, utilizing architectures that range
16 from temporal convolutions [1] to 3D convolutions [2, 3] and, more recently, transformers [4, 5]. The
17 current trend towards scaling has led to the emergence of multi-modal foundation models [6, 7, 8],
18 which represent the state-of-the-art in video understanding [9, 10, 11, 12, 13, 14]. These models are
19 trained on massive amounts of web data, demonstrating exceptional generalization capabilities across
20 different tasks. Additionally, they can engage in open-vocabulary, multi-round interactions with users,
21 a capability that previous specialized models lacked [9, 12, 14]. This advancement holds significant
22 promise for real-world applications, such as personal assistants.

23 Despite the progress, current video foundation models process videos differently from humans.
24 Typically, these models use one of two approaches. The first approach (top left of Figure 1) involves
25 sparsely sampling frames from the input video and only processing those sampled frames [9, 10,
26 11, 12, 13, 14]. The second approach (top right of Figure 1) divides the input video into separate
27 chunks, processes each chunk independently by captioning it, and then summarizes the entire video’s
28 information by using a large language model (LLM) to process the generated captions [15, 16, 17].
29 In contrast, humans perceive and process visual signals densely and continuously. We anticipate that
30 the next generation of visual foundation models should mimic this human approach, processing input
31 video comprehensively without resorting to sparse sampling or dividing it into chunks. Firstly, sparse
32 sampling or chunk processing can result in the loss of global temporal information across the entire
33 video. More importantly, we believe that the ability to continuously process visual signals efficiently
34 is crucial for learning critical concepts such as compositionality [18], intuitive physics [19], and

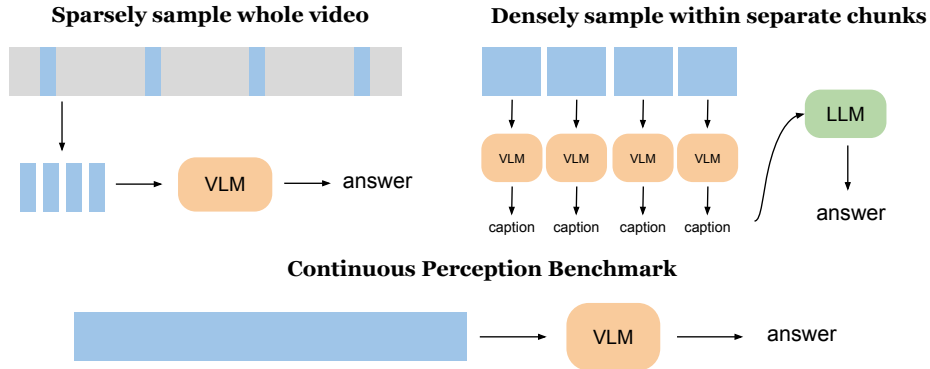


Figure 1: (Top) Existing video understanding models process videos in one of two ways: either by sparsely processing the entire video or by densely processing it in chunks. Similarly, most existing video benchmarks can be addressed using these approaches, as the information needed to answer questions can either be sparsely extracted from the entire video or found within a local region of the video. (Bottom) We propose the Continuous Perception Benchmark, a task that requires models to densely process input videos to answer questions correctly. We hope this task could facilitate the development of the next generation of vision models that emulate human ability to continuously perceive and process visual signals.

35 object permanence [20], as processing only a small number of frames may lead to learning superficial
 36 or spurious shortcut signals [21]. Additionally, such models could leverage the massive amount of
 37 available online video content for learning, which existing video models cannot do effectively due to
 38 excessive costs.

39 To facilitate the development of this envisioned next generation of vision models, we propose a
 40 new benchmark, called Continuous Perception Benchmark. This benchmark differs from existing
 41 video benchmarks [22, 23] by requiring models to continuously analyze the entire video stream for
 42 optimal performance (bottom of Figure 1). Most existing video benchmarks can often be tackled
 43 by analyzing just key frames [24, 25, 26, 11] or processing the video in segments [4, 22, 23].
 44 However, the Continuous Perception Benchmark pushes models to develop a more comprehensive
 45 and uninterrupted understanding of the video. We evaluated several state-of-the-art foundational
 46 video models [15, 27, 11, 12, 15, 10, 11], both open-sourced and commercial, and found that none of
 47 them performed well on this newly proposed task. For instance, the best-performing model could
 48 only correctly answer 12% of the questions without any errors. This highlights the limitations of
 49 existing models and underscores the need for developing new techniques in this area.

50 2 Related Work

51 2.1 Multi-modal Foundational Models

52 The advent of multi-modal foundational models has marked a significant breakthrough in the field
 53 of artificial intelligence, enabling the integration of diverse data modalities such as text, images,
 54 and videos. In this paper we benchmark the open-sourced models and models with a public API:
 55 Video-ChatGPT [9], VideoLLaVa [10], LLoVi [15], PLLaVA [12], VideoChat2 [11], and Gemini [27].
 56 Video-ChatGPT [9] computes spatiotemporal features from the videos by averaging frame-level
 57 features across temporal and spatial features, as input to the LLM through a learnable linear layer.
 58 VideoLLaVa [10] aligns images and videos before projection, enabling the LLM to learn from a
 59 unified visual representation. This process allows the LLM to comprehend both images and videos
 60 simultaneously. LLoVi [15] employs short-term visual captioners (such as LaViLa and BLIP2) to
 61 create textual descriptions for brief video segments. An LLM then compiles these detailed, short-term
 62 captions to perform the long-range reasoning necessary for LVQA. This approach enables LLoVi to
 63 effectively manage long-duration videos. PLLaVA [12] employs a simple pooling strategy to smooth

64 the feature distribution along the temporal dimension as input to the LLM. VideoChat2 [11] bridges
65 LLM with a powerful vision foundational model [28], and trains the model on diverse instruction-
66 tuning data with a novel progressive training paradigm. Gemini [27] is jointly trained across image,
67 audio, video, and text data for the purpose of building a model with strong generalist capabilities
68 across modalities.

69 **2.2 Video Benchmarks**

70 Various video benchmarks have been introduced over the years to advance video understanding
71 technologies [25, 29, 30]. Early benchmarks focused on specific tasks such as activity classifica-
72 tion [24, 25, 26], motion understanding [31], or movie analysis [32]. With the advent of visual
73 foundation models [8, 6, 7, 9, 10], recent benchmarks have become more comprehensive, evaluating
74 a wide range of model capabilities [33, 11] and often sourcing data from multiple existing video
75 benchmarks [11, 34]. Another trend in benchmarking focuses on assessing long-form video under-
76 standing abilities [4, 22, 23]. Despite these diverse approaches, most existing benchmarks fall into
77 two categories, where the information for answering the question can be extracted by either sparsely
78 sampling several key frames [24, 25, 26, 11], or by captioning each small segments independently and
79 then summarizing the resulting captions with language models [4, 22, 23]. Our proposed benchmark
80 stands apart, as it requires the model to continuously process the entire input video. The information
81 needed to answer the questions is densely distributed throughout the video, demanding continuous
82 perception of visual stimuli as humans do.

83 **2.3 Synthetic Datasets in Computer Vision**

84 Our work, which involves synthetically generated data, is closely related to other research in computer
85 vision. Their primary focus is to employ synthetic training data for real-world applications such as
86 optical flow [35], point tracking [36], scene understanding [37, 38], and human pose understand-
87 ing [39, 40, 41]. Another use of synthetic datasets is to investigate model capabilities in controlled
88 environments. For spatial reasoning, some studies [42] render predefined objects using softwares
89 like Blender [43]. More recently, research focusing on embodied agents has leveraged advanced
90 simulators [44, 45] to create realistic environments. These simulators are equipped with a wide
91 variety of assets and use physics engines like PyBullet [46] to generate more accurate and physically
92 plausible scenes. This approach allows for a detailed examination of models’ abilities in settings that
93 closely mimic real-world conditions.

94 **3 Continuous Perception Benchmark**

95 To fill in the gap of existing benchmarks, Continuous Perception Benchmark (CPB) aims to build a
96 video question and answering dataset that requires continuous processing of video frames. We use it
97 to benchmark multi-modal foundational models to assess their capabilities for continuous perception.

98 **3.1 Generation Method**

99 We curate the dataset using OmniGibson [45] (MIT License), a simulation environment built upon
100 NVIDIA’s Omniverse platform. We select a 3D scene and populate it with furniture such as chairs and
101 tables, then randomly place objects on the tables. Then videos are rendered with a moving camera
102 following a specific trajectory (Figure 2). The task is simply asking how many of a specific objects
103 are shown in the input video. Despite its simplicity, in the experiment section we show none of the
104 existing state-of-the-art video models can perform well on the task.

105 The basic version of the dataset is created by having a camera move at a consistent speed across a room,
106 maintaining a fixed direction to capture a panoramic view. This process results in a 20-second video
107 at 30 fps for each instance. This method ensures that the visual data encompasses a continuous and
108 seamless sweep of the entire room, providing comprehensive spatial context. To answer questions like

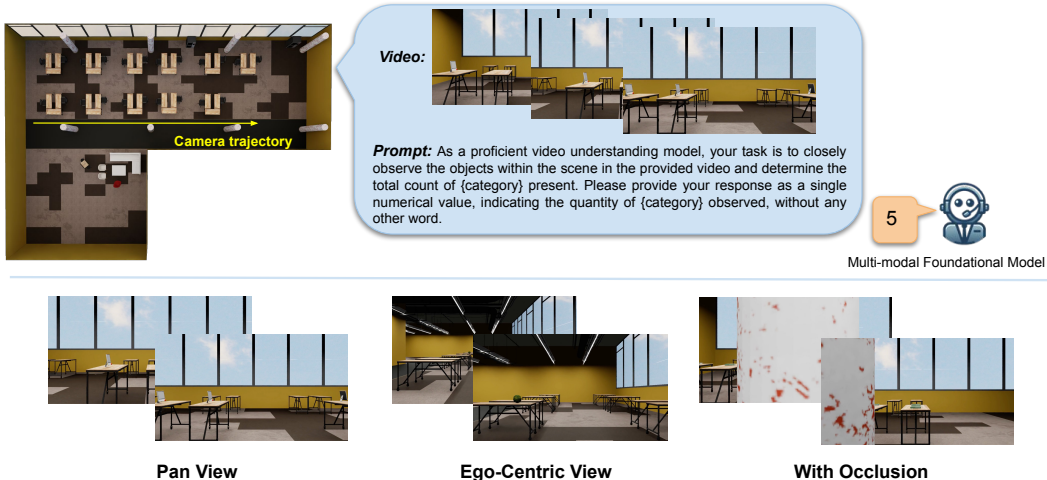


Figure 2: Top: Data generation (left) and benchmarking (right) illustration. Bottom: different variations of the benchmark.

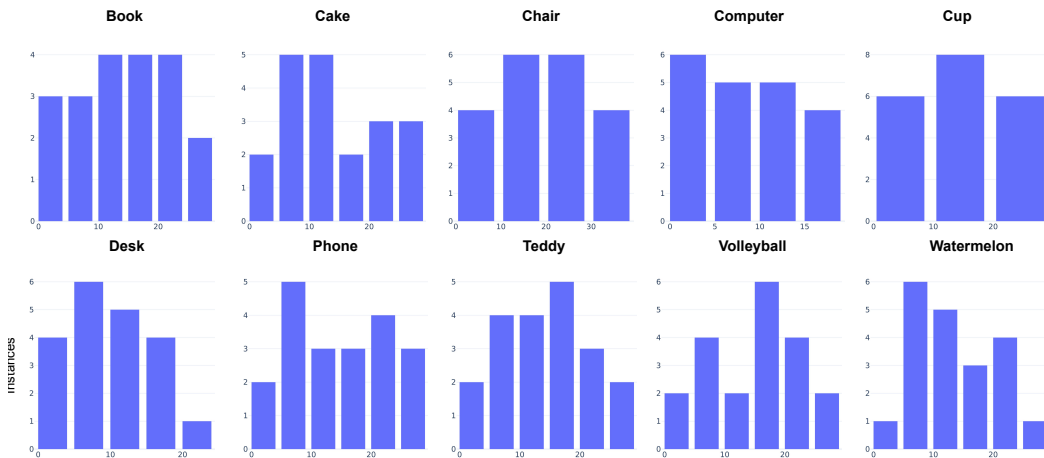


Figure 3: Groundtruth count distribution for different target categories.

109 "how many desks are there in the room?", the model must thoroughly understand spatial relationships
 110 and environmental context, which requires processing the input video densely and continuously.

111 We select 10 object categories from the Behavior-1K database [45]: book, cake, chair, computer, cup,
 112 desk, phone, teddy bear, volleyball, and watermelon. For each category, we randomly sample 20
 113 different scene configurations with different number of target object present at different locations,
 114 resulting a total of 200 test instances. Figure 3 shows the distributions of the ground truth count for
 115 different categories, which are roughly evenly represented across counts ranging from 1 to 30.

116 3.2 Evaluation Method

117 Following previous repetition counting works [47, 48, 49, 50], we use Mean Absolute Error (MAE),
 118 Root-Mean-Square-Error (RMSE), Off-By-One accuracy (OBO), Off-By-Zero (OBZ) as evaluation
 119 metrics, calculated as Eqs. 1 and 2 respectively. We additionally report Off-By-Five (OBF) accuracy
 120 (Eq. 3). The metrics OBF, OBO, and OBZ exhibit increasing levels of stringency for precise count
 121 accuracy. RMSE is more robust for evaluating diverse counts, as it is less biased towards smaller

122 counts compared to MAE.

$$MAE = \frac{1}{|\Omega|} \sum_{i \in \Omega} \frac{|c_i - \tilde{c}_i|}{c_i} \quad ; \quad RMSE = \sqrt{\frac{1}{|\Omega|} \sum_{i \in \Omega} (c_i - \tilde{c}_i)^2} \quad (1)$$

123

$$OBZ = \frac{1}{|\Omega|} \sum_{i \in \Omega} \mathbb{1}(|c_i - \tilde{c}_i| \leq 0) \quad ; \quad OBO = \frac{1}{|\Omega|} \sum_{i \in \Omega} \mathbb{1}(|c_i - \tilde{c}_i| \leq 1) \quad (2)$$

124

$$OBF = \frac{1}{|\Omega|} \sum_{i \in \Omega} \mathbb{1}(|c_i - \tilde{c}_i| \leq 5) \quad (3)$$

125 c_i, \tilde{c}_i are the ground-truth and predicted counts for i_{th} video in the dataset Ω . $\mathbb{1}$ is the indicator
126 function.

127 4 Experiments

128 In this section, we will first introduce the various baseline models we evaluated on the proposed
129 continuous perception benchmark. Then, we will present the experiment results and provide a detailed
130 analysis of the model predictions.

131 4.1 Baselines

132 We evaluated several models aimed at video understanding. Specifically, Video-LLaVA [10],
133 PLLaVA [12], VideoChat2 [11], and Video-ChatGPT [9] represent open-source multimodal models
134 that generate answers directly from input video and question descriptions. LLoVi [15] represents
135 models that first caption small, separate chunks of the input video, then summarize the captions of
136 all chunks, and answer the question using a large language model (LLM). For commercial models,
137 we evaluated Gemini [27] from Google. For all the open-source models, we utilized the inference
138 code and released checkpoints from the official implementations. Figure 4 summarizes prompts
139 used for different models, we used the ‘VLM Prompt’ for Video-LLaVA, PLLaVA, VideoChat2,
140 Video-ChatGPT, and Gemini, and ‘Captioning Prompt’, ‘LLM Prompt’ for captioning part and
141 answer generation part for LLoVi respectively. Note that we made small changes to the captioning
142 prompt for LLoVi to deliberately instruct the captioning to output specific quantities of the target
143 object. All open-source models are evaluated on an A6000 server.

144 **Video-LLaVA [10].** Video-LLaVA represents a simple and robust multi-modal foundation model
145 baseline where the visual representation is aligned with feature space of a large language model
146 resulting in a unified large vision-language model. The model is trained on a mixed of image and
147 video datasets where the image and video are first aligned before projecting to language feature space.
148 It operates on input videos by sampling eight frames.

149 **PLLaVA [12].** PLLaVA employs a simple pooling strategy to smooth the feature distribution along
150 the temporal dimension as input to the LLM. This is shown to effectively reduce the dominant impacts
151 from the extreme features. Our experiments were conducted using the 7B version of the model. When
152 processing videos, PLLaVA samples 16 frames at a resolution of 336.

153 **VideoChat2 [11].** VideoChat2 introduces a progressive training approach that incorporates a diverse
154 range of multimodal instructions. This method effectively aligns video and language modalities.
155 Our experiment utilized the 7B version of the model, processing input videos with 16 frames at a
156 resolution of 224.

157 **Video-ChatGPT [9].** Video-ChatGPT leverages CLIP-L/14 as the visual encoder to extract both
158 spatial and temporal video features and the spatiotemporal features are computed through averaging
159 frame-level features across temporal and spatial dimensions respectively. It sample the input video
160 with 100 frames at resolution 224.

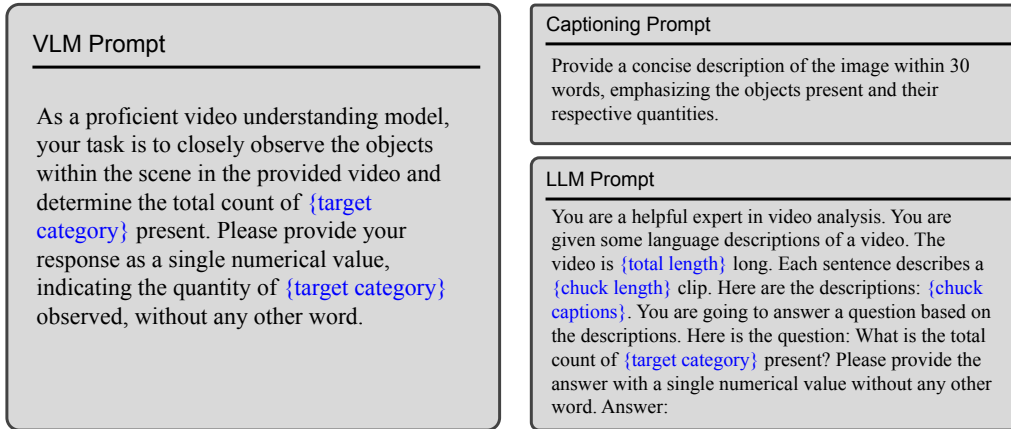


Figure 4: Prompts used for different models.

161 **LLoVi [15].** LLoVi is a framework designed for Long-Range Video Question Answering (LVQA).
 162 This method consists of two stages: initially, short-term visual captioners (such as LaViLa and BLIP2)
 163 generate textual descriptions for brief video segments spanning from 0.5 to 8 seconds. Subsequently,
 164 a Large Language Model (LLM) consolidates these short-term captions and conducts long-range
 165 reasoning. In our experiment, we employed BLIP2 for captioning and Llama-7B for summarizing the
 166 captions and answering the questions.

167 **Gemini [27].** Gemini is a family of highly capable multimodal models developed by Google.
 168 Gemini models are trained jointly across image, audio, video and text data for strong generalist
 169 capabilities across modalities. We tested Gemini-1.5-Flash and Gemini-1.5-Pro version on our
 170 proposed benchmark.

171 4.2 Experiment Results

172 Table 1 summarizes the overall evaluation results across different metrics. Notably, all models
 173 perform poorly on the proposed benchmark. Specifically, the best model, Gemini-1.5-Flash, correctly
 174 answers the questions only 12% of the time (OBZ). The predicted count is within one of the ground
 175 truth (OBO) only 20% of the time, and within five (OBF) 52% of the time. The mean absolute
 176 error (MAE) and root mean square error (RMSE) are also high, at 0.5 and 8.54, respectively. The
 177 performance of other open-source models is even worse, with OBO as low as 6% and RMSE as high
 178 as 14 (Video-LLaVA). This indicates that none of the existing video models can successfully complete
 179 the proposed task, which requires continuously modeling the entire input video and aggregating
 180 information perceived over time. Among the open-source models, LLoVi performs the best, with
 181 an OBF greater than 50% (compared to less than 45% for the others) and an RMSE lower than
 182 9 (while others are higher than 11.5). This superior performance may be attributed to LLoVi’s
 183 approach of dividing the input video into chunks and captioning each chunk, allowing it to process
 184 more input frames than the other models. Table 2 details the MAE for each object category. It
 185 shows that performance of different models varies across categories. For instance, LLoVi performs
 186 relatively better on ‘watermelon’ (0.28) than on ‘cake’ (0.44), while Gemini-1.5-Flash shows better
 187 performance on ‘cake’ (0.28) than on ‘watermelon’ (0.40).

188 **Distribution of predicted counts.** To further understand the models’ predictions, we plot the
 189 distribution of predicted counts for each model, as shown in Figure 5. For Video-LLaVA and
 190 PLLaVA, most predicted counts are under 5, including cases where the model outputs a sentence
 191 without a valid number, which we set to 0. Video-ChatGPT’s answers mostly fall under 2 and between
 192 10-15. LLoVi predicts most answers under 20, while Gemini predicts most answers under 15. Most
 193 surprisingly, VideoChat2 almost always predicts counts within the 10-12 range. The striking disparity

Table 1: Overall results for different models.

Model	OBZ	OBO	OBF	MAE	RMSE	CORR
Video-LLaVA	0.01	0.06	0.23	0.87	14.07	0.43
PLLaVA	0.03	0.10	0.29	0.76	12.64	0.45
VideoChat2	0.04	0.12	0.43	1.03	12.17	0.31
Video-ChatGPT	0.02	0.10	0.33	1.04	11.86	0.11
LLoVi	0.04	0.17	0.53	0.78	8.86	0.45
Gemini-1.5-Flash	0.12	0.20	0.52	0.50	8.54	0.72
Gemini-1.5-Pro	0.06	0.15	0.45	0.52	9.01	0.83

Table 2: Mean Absolute Error (MAE) of different models for all categories.

Model	BO	CA	CH	CO	CU	DE	PH	TE	VO	WA	All
Video-LLaVA	0.98	0.87	0.68	1.03	0.93	0.65	0.89	0.89	0.90	0.91	0.87
PLLaVA	1.00	0.79	0.54	0.79	0.90	0.45	0.95	0.59	0.82	0.77	0.76
VideoChat2	1.29	0.88	1.39	1.25	1.08	1.39	0.89	0.99	0.62	0.54	1.03
Video-ChatGPT	1.42	0.83	1.09	1.01	1.25	0.68	1.35	1.01	0.61	1.16	1.04
LLoVi	0.87	0.44	0.95	1.60	1.08	0.76	1.06	0.30	0.47	0.28	0.78
Gemini-1.5-Flash	0.22	0.28	0.77	0.76	0.81	0.51	0.51	0.30	0.46	0.40	0.50
Gemini-1.5-Pro	0.45	0.39	0.76	0.72	0.49	0.38	0.60	0.38	0.55	0.45	0.52

194 between the predicted count distribution and the ground truth count distribution (shown on the left
 195 side of Figure 3) raises the question: "Does the model ever make predictions based on the input
 196 video?" To investigate this, we calculate the correlation between predicted counts and ground truth
 197 counts and summarize the results in the rightmost column of Table 1. The analysis reveals that,
 198 except for two Gemini models, which show a correlation of 0.72 and 0.83 for 1.5-Flash and 1.5-Pro
 199 respectively, all other models' predictions have a correlation with the ground truth of less than 0.5.
 200 This is the case despite LLoVi demonstrating similar performance to Gemini models on OBF and
 201 RMSE metrics.

202 **Distribution of correct predictions.** Figure 6 illustrates the percentage of correct predictions made
 203 by Gemini-1.5-Flash for each ground-truth count, as measured by OBZ, OBO, and OBF. The model
 204 demonstrates relatively better accuracy when the ground-truth count is low. However, when there are
 205 more than 8 target objects, the best OBO is less than 30%. This is understandable because higher
 206 ground-truth counts imply that objects are likely spread across different times rather than being

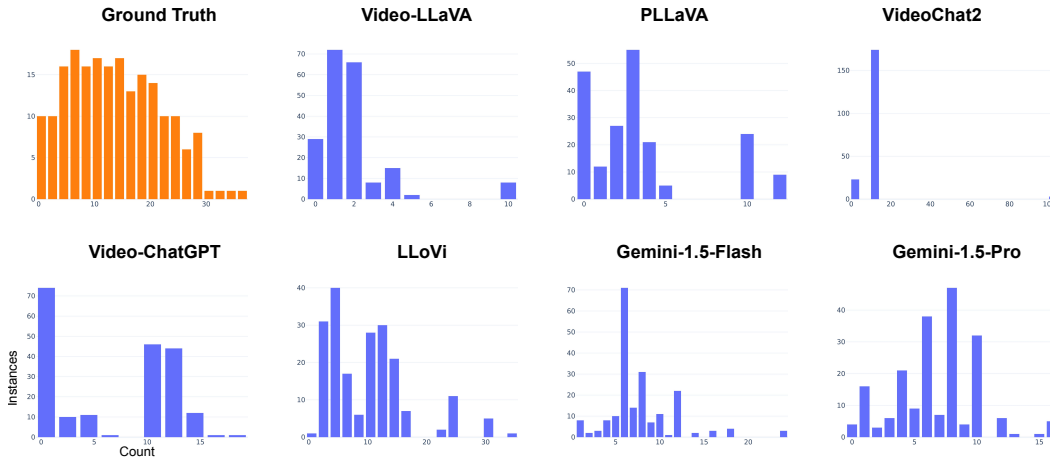


Figure 5: Predicted count distribution for different models.

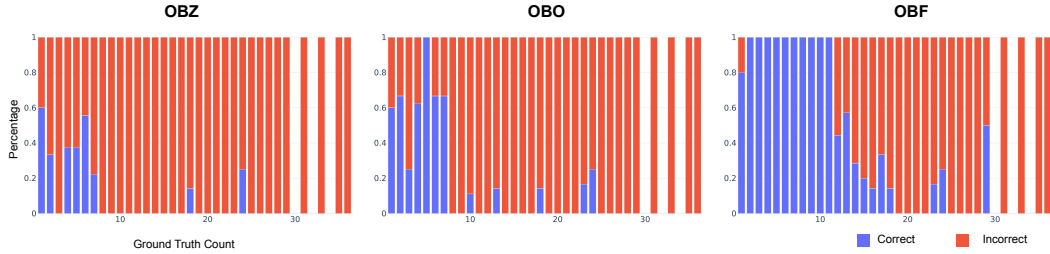


Figure 6: Distribution of correct prediction for Gemini-1.5-Flash. It shows that the model performs well when the ground truth count is low but struggles when there are more than 10 target objects in the scene.

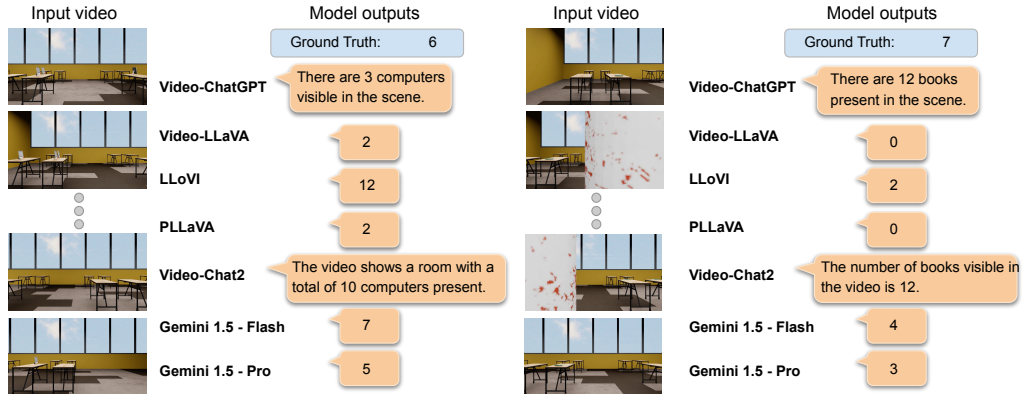


Figure 7: Examples from the proposed benchmark as well as the models’ generated answer. Despite explicit instructions to output only a single number, some models still produce a complete sentence. When this occurs, we extract the first number from the output sentence as the model’s prediction. If no number is present in the sentence, we set the prediction to zero.

207 concentrated in a local region. This situation requires the integration of a longer temporal context,
 208 which the model struggles to achieve effectively.

209 **4.3 Additional Experiments**

210 All experiments presented in the previous sections were conducted on the base version of the dataset,
 211 where the total length of the video is 20 seconds and the camera moves at a uniform speed. In this
 212 section, we conduct experiments with different variations of the base dataset. Table 3 summarizes the
 213 results of the Gemini-1.5-Flash model.

214 **With occlusion.** To simulate real-world scenarios where objects or structures can temporarily block
 215 the line of sight, we place pillars within the room. As the camera moves across the room, these pillars
 216 periodically obstruct the view, resulting in some frames being occluded (Bottom right of Figure 2).
 217 The occlusions challenge models to infer and reason about the environment despite partial visibility,
 218 testing their robustness and capability to handle incomplete or obstructed visual data. Despite the
 219 added difficulty, Gemini-1.5-Flash shows similar performance to the base version, indicating that
 220 additional occlusion does not influence the model’s predictions.

221 **Nonuniform camera speed.** Furthermore, to explicitly discourage models from employing sparse
 222 uniform sampling, we introduce variations in the speed of the camera movement. Specifically, instead
 223 of using a uniform camera speed, we randomly sample from one of three movement patterns: starting
 224 fast and then slowing down, starting slow and then speeding up, or starting with a speedup followed

Table 3: Performance of Gemini-1.5-Flash on different variations of the dataset. ‘Base’ is the setting where the camera moves at a constant speed and captures a 20-second third-person view. ‘Occlusion’ introduces an additional foreground object, resulting in occlusion. ‘Nonuniform’ varies the camera speed. ‘5s Length’ and ‘2min Length’ are versions with total video lengths of 5 seconds and 2 minutes, respectively. ‘Egocentric’ is the setting where the camera captures the first-person view. The model is not sensitive to foreground occlusion. It performs worse on the nonuniform 5s and 20s settings, but shows better results on the egocentric and nonuniform 2min settings.

Model	OBZ	OBO	OBF	MAE	RMSE	CORR
Base	0.12	0.20	0.52	0.50	8.54	0.72
Occlusion	0.10	0.21	0.52	0.50	8.48	0.77
Nonuniform Speed	0.09	0.17	0.48	0.51	8.92	0.75
5s Length	0.04	0.11	0.37	0.65	10.70	0.74
2min Length	0.10	0.23	0.59	0.45	7.59	0.75
Egocentric	0.10	0.27	0.64	0.54	6.16	0.70

225 by a slowdown. Compared to base version, Gemini performs slightly worse in this setting, with the
 226 OBF dropping from 54% to 48%, and the RMSE increasing from 8.54 to 8.92.

227 **Video lengths.** The base version of the dataset has a fixed length of 20 seconds. We also experimented
 228 with two versions with different total lengths: one at 5 seconds and one at 2 minutes. Note that
 229 for both of the versions, the camera speed is not constant as in the ‘nonuniform speed’ version.
 230 Gemini shows a relatively large performance degradation on the 5-second large version, with the OBF
 231 decreasing from 52% to 37% and the MAE increasing from 0.5 to 0.65. This might indicate that
 232 Gemini processes videos with a fixed frames-per-second rate, resulting in insufficient frame sampling
 233 for the 5-second dataset. For the 2-minute version, the model shows a slight decrease in performance
 234 in OBZ but improved performance in all other metrics.

235 **Egocentric view.** Finally, we created a variation of the dataset with an egocentric view instead of a
 236 third-person view, as this is common in many real-world applications such as home robots. On this
 237 dataset, Gemini shows improved OBF (from 52% to 64%) and RMSE (from 8.54 to 6.16). This could
 238 suggest that the model might have a better spatial understanding when processing an egocentric view
 239 compared to a third-person view.

240 5 Conclusion

241 In summary, we introduce a novel benchmark called the Continuous Perception Benchmark. The
 242 key distinction of this benchmark is that, to answer questions correctly, models must densely process
 243 the entire video, in contrast to existing benchmarks where sparse sampling or processing video in
 244 chunks is sufficient. Evaluation of multiple state-of-the-art video foundation models demonstrates
 245 that none of them excel at this task, indicating the need for new techniques. We hope this benchmark
 246 could facilitate developing the next generation of vision models that mimic human capabilities to
 247 continuously perceive and process visual stimuli. This advancement could be crucial for acquiring
 248 essential knowledge such as compositionality, intuitive physics, and object permanence.

249 **Limitations and future work.** One limitation of the dataset is its synthetic nature, which may
 250 present challenges when transferring models from simulation to real-world scenarios. However, our
 251 experiments indicate that existing models struggle to handle even synthetic data effectively. Future
 252 work could consider collecting more real-world data to improve the diversity of the datasets.

253 **Potential negative societal impacts.** This paper introduces a challenging task along with bench-
 254 marked performance of multi-modal foundational models, aiming to enhance the continuous percep-
 255 tion capabilities of video foundational models. While we emphasize responsible use, we acknowledge
 256 the potential for these powerful video understanding models to be exploited for malicious purposes,
 257 such as unauthorized surveillance and automated profiling.

258 References

- 259 [1] Andrej Karpathy, George Toderici, Sanketh Shetty, Thomas Leung, Rahul Sukthankar, and Li Fei-Fei.
260 Large-scale video classification with convolutional neural networks. In *Proceedings of the IEEE conference*
261 *on Computer Vision and Pattern Recognition*, pages 1725–1732, 2014.
- 262 [2] Saining Xie, Chen Sun, Jonathan Huang, Zhuowen Tu, and Kevin Murphy. Rethinking spatiotemporal
263 feature learning for video understanding. *arXiv preprint arXiv:1712.04851*, 1(2):5, 2017.
- 264 [3] Hengduo Li, Zuxuan Wu, Abhinav Shrivastava, and Larry S Davis. 2d or not 2d? adaptive 3d convolution
265 selection for efficient video recognition. In *Proceedings of the IEEE/CVF conference on computer vision*
266 *and pattern recognition*, pages 6155–6164, 2021.
- 267 [4] Chao-Yuan Wu and Philipp Krahenbuhl. Towards long-form video understanding. In *Proceedings of the*
268 *IEEE/CVF Conference on Computer Vision and Pattern Recognition*, pages 1884–1894, 2021.
- 269 [5] Shen Yan, Xuehan Xiong, Anurag Arnab, Zhichao Lu, Mi Zhang, Chen Sun, and Cordelia Schmid.
270 Multiview transformers for video recognition. In *Proceedings of the IEEE/CVF conference on computer*
271 *vision and pattern recognition*, pages 3333–3343, 2022.
- 272 [6] Alec Radford, Jong Wook Kim, Chris Hallacy, Aditya Ramesh, Gabriel Goh, Sandhini Agarwal, Girish
273 Sastry, Amanda Askell, Pamela Mishkin, Jack Clark, et al. Learning transferable visual models from
274 natural language supervision. In *International conference on machine learning*, pages 8748–8763. PMLR,
275 2021.
- 276 [7] Mathilde Caron, Hugo Touvron, Ishan Misra, Hervé Jégou, Julien Mairal, Piotr Bojanowski, and Armand
277 Joulin. Emerging properties in self-supervised vision transformers. In *Proceedings of the IEEE/CVF*
278 *international conference on computer vision*, pages 9650–9660, 2021.
- 279 [8] Haotian Liu, Chunyuan Li, Qingyang Wu, and Yong Jae Lee. Visual instruction tuning. *Advances in neural*
280 *information processing systems*, 36, 2024.
- 281 [9] Muhammad Maaz, Hanoona Rasheed, Salman Khan, and Fahad Shahbaz Khan. Video-chatgpt: Towards
282 detailed video understanding via large vision and language models. *arXiv preprint arXiv:2306.05424*,
283 2023.
- 284 [10] Bin Lin, Bin Zhu, Yang Ye, Munan Ning, Peng Jin, and Li Yuan. Video-llava: Learning united visual
285 representation by alignment before projection. *arXiv preprint arXiv:2311.10122*, 2023.
- 286 [11] Kunchang Li, Yali Wang, Yinan He, Yizhuo Li, Yi Wang, Yi Liu, Zun Wang, Jilan Xu, Guo Chen, Ping
287 Luo, et al. Mvbench: A comprehensive multi-modal video understanding benchmark. *arXiv preprint*
288 *arXiv:2311.17005*, 2023.
- 289 [12] Lin Xu, Yilin Zhao, Daquan Zhou, Zhijie Lin, See Kiong Ng, and Jiashi Feng. Pllava: Parameter-free llava
290 extension from images to videos for video dense captioning. *arXiv preprint arXiv:2404.16994*, 2024.
- 291 [13] Yi Wang, Kunchang Li, Yizhuo Li, Yinan He, Bingkun Huang, Zhiyu Zhao, Hongjie Zhang, Jilan Xu,
292 Yi Liu, Zun Wang, et al. Internvideo: General video foundation models via generative and discriminative
293 learning. *arXiv preprint arXiv:2212.03191*, 2022.
- 294 [14] Yi Wang, Kunchang Li, Xinhao Li, Jiashuo Yu, Yinan He, Guo Chen, Baoqi Pei, Rongkun Zheng, Jilan
295 Xu, Zun Wang, et al. Internvideo2: Scaling video foundation models for multimodal video understanding.
296 *arXiv preprint arXiv:2403.15377*, 2024.
- 297 [15] Ce Zhang, Taixi Lu, Md Mohaiminul Islam, Ziyang Wang, Shoubin Yu, Mohit Bansal, and Gedas Bertasius.
298 A simple llm framework for long-range video question-answering. *arXiv preprint arXiv:2312.17235*, 2023.
- 299 [16] Chuyi Shang, Amos You, Sanjay Subramanian, Trevor Darrell, and Roei Herzig. Traveler: A multi-llm
300 agent framework for video question-answering. *arXiv preprint arXiv:2404.01476*, 2024.
- 301 [17] Ying Wang, Yanlai Yang, and Mengye Ren. Lifelongmemory: Leveraging llms for answering queries in
302 egocentric videos. *arXiv preprint arXiv:2312.05269*, 2023.
- 303 [18] Klaus Greff, Sjoerd Van Steenkiste, and Jürgen Schmidhuber. On the binding problem in artificial neural
304 networks. *arXiv preprint arXiv:2012.05208*, 2020.
- 305 [19] Brenden M Lake, Tomer D Ullman, Joshua B Tenenbaum, and Samuel J Gershman. Building machines
306 that learn and think like people. *Behavioral and brain sciences*, 40:e253, 2017.

- 307 [20] Elizabeth S Spelke and Katherine D Kinzler. Core knowledge. *Developmental science*, 10(1):89–96, 2007.
- 308 [21] Robert Geirhos, Jörn-Henrik Jacobsen, Claudio Michaelis, Richard Zemel, Wieland Brendel, Matthias
309 Bethge, and Felix A Wichmann. Shortcut learning in deep neural networks. *Nature Machine Intelligence*,
310 2(11):665–673, 2020.
- 311 [22] Junbin Xiao, Xindi Shang, Angela Yao, and Tat-Seng Chua. Next-qa: Next phase of question-answering to
312 explaining temporal actions. In *Proceedings of the IEEE/CVF conference on computer vision and pattern
313 recognition*, pages 9777–9786, 2021.
- 314 [23] Karttikeya Mangalam, Raiymbek Akshulakov, and Jitendra Malik. Egoschema: A diagnostic benchmark
315 for very long-form video language understanding. *Advances in Neural Information Processing Systems*,
316 36, 2024.
- 317 [24] Khurram Soomro, Amir Roshan Zamir, and Mubarak Shah. Ucf101: A dataset of 101 human actions
318 classes from videos in the wild. *arXiv preprint arXiv:1212.0402*, 2012.
- 319 [25] Will Kay, Joao Carreira, Karen Simonyan, Brian Zhang, Chloe Hillier, Sudheendra Vijayanarasimhan,
320 Fabio Viola, Tim Green, Trevor Back, Paul Natsev, et al. The kinetics human action video dataset. *arXiv
321 preprint arXiv:1705.06950*, 2017.
- 322 [26] Joao Carreira and Andrew Zisserman. Quo vadis, action recognition? a new model and the kinetics dataset.
323 In *proceedings of the IEEE Conference on Computer Vision and Pattern Recognition*, pages 6299–6308,
324 2017.
- 325 [27] Gemini Team, Rohan Anil, Sebastian Borgeaud, Yonghui Wu, Jean-Baptiste Alayrac, Jiahui Yu, Radu
326 Soricut, Johan Schalkwyk, Andrew M Dai, Anja Hauth, et al. Gemini: a family of highly capable
327 multimodal models. *arXiv preprint arXiv:2312.11805*, 2023.
- 328 [28] Kunchang Li, Yali Wang, Yizhuo Li, Yi Wang, Yanan He, Limin Wang, and Yu Qiao. Unmasked teacher:
329 Towards training-efficient video foundation models. In *Proceedings of the IEEE/CVF International
330 Conference on Computer Vision*, pages 19948–19960, 2023.
- 331 [29] Joao Carreira, Eric Noland, Andras Banki-Horvath, Chloe Hillier, and Andrew Zisserman. A short note
332 about kinetics-600. *arXiv preprint arXiv:1808.01340*, 2018.
- 333 [30] Joao Carreira, Eric Noland, Chloe Hillier, and Andrew Zisserman. A short note on the kinetics-700 human
334 action dataset. *arXiv preprint arXiv:1907.06987*, 2019.
- 335 [31] Raghav Goyal, Samira Ebrahimi Kahou, Vincent Michalski, Joanna Materzynska, Susanne Westphal,
336 Heuna Kim, Valentin Haenel, Ingo Fruend, Peter Yianilos, Moritz Mueller-Freitag, et al. The "something
337 something" video database for learning and evaluating visual common sense. In *Proceedings of the IEEE
338 international conference on computer vision*, pages 5842–5850, 2017.
- 339 [32] Dejing Xu, Zhou Zhao, Jun Xiao, Fei Wu, Hanwang Zhang, Xiangnan He, and Yueting Zhuang. Video
340 question answering via gradually refined attention over appearance and motion. In *Proceedings of the 25th
341 ACM international conference on Multimedia*, pages 1645–1653, 2017.
- 342 [33] Viorica Patraucean, Lucas Smaira, Ankush Gupta, Adria Recasens, Larisa Markeeva, Dylan Banarse,
343 Skanda Koppula, Mateusz Malinowski, Yi Yang, Carl Doersch, et al. Perception test: A diagnostic
344 benchmark for multimodal video models. *Advances in Neural Information Processing Systems*, 36, 2024.
- 345 [34] Munan Ning, Bin Zhu, Yujia Xie, Bin Lin, Jiayi Cui, Lu Yuan, Dongdong Chen, and Li Yuan. Video-bench:
346 A comprehensive benchmark and toolkit for evaluating video-based large language models. *arXiv preprint
347 arXiv:2311.16103*, 2023.
- 348 [35] Daniel J Butler, Jonas Wulff, Garrett B Stanley, and Michael J Black. A naturalistic open source movie for
349 optical flow evaluation. In *Computer Vision–ECCV 2012: 12th European Conference on Computer Vision,
350 Florence, Italy, October 7–13, 2012, Proceedings, Part VI 12*, pages 611–625. Springer, 2012.
- 351 [36] Yang Zheng, Adam W Harley, Bokui Shen, Gordon Wetzstein, and Leonidas J Guibas. Pointodyssey: A
352 large-scale synthetic dataset for long-term point tracking. In *Proceedings of the IEEE/CVF International
353 Conference on Computer Vision*, pages 19855–19865, 2023.
- 354 [37] Shuran Song, Fisher Yu, Andy Zeng, Angel X Chang, Manolis Savva, and Thomas Funkhouser. Semantic
355 scene completion from a single depth image. In *Proceedings of the IEEE conference on computer vision
356 and pattern recognition*, pages 1746–1754, 2017.

- 357 [38] Stephan R Richter, Zeeshan Hayder, and Vladlen Koltun. Playing for benchmarks. In *Proceedings of the*
358 *IEEE International Conference on Computer Vision*, pages 2213–2222, 2017.
- 359 [39] Gul Varol, Javier Romero, Xavier Martin, Naureen Mahmood, Michael J Black, Ivan Laptev, and Cordelia
360 Schmid. Learning from synthetic humans. In *Proceedings of the IEEE conference on computer vision and*
361 *pattern recognition*, pages 109–117, 2017.
- 362 [40] Priyanka Patel, Chun-Hao P Huang, Joachim Tesch, David T Hoffmann, Shashank Tripathi, and Michael J
363 Black. Agora: Avatars in geography optimized for regression analysis. In *Proceedings of the IEEE/CVF*
364 *Conference on Computer Vision and Pattern Recognition*, pages 13468–13478, 2021.
- 365 [41] Michael J Black, Priyanka Patel, Joachim Tesch, and Jinlong Yang. Bedlam: A synthetic dataset of bodies
366 exhibiting detailed lifelike animated motion. In *Proceedings of the IEEE/CVF Conference on Computer*
367 *Vision and Pattern Recognition*, pages 8726–8737, 2023.
- 368 [42] Rohit Girdhar and Deva Ramanan. Cater: A diagnostic dataset for compositional actions and temporal
369 reasoning. *arXiv preprint arXiv:1910.04744*, 2019.
- 370 [43] Blender Online Community. *Blender - a 3D modelling and rendering package*. Blender Foundation,
371 Stichting Blender Foundation, Amsterdam, 2018. URL <http://www.blender.org>.
- 372 [44] Eric Kolve, Roozbeh Mottaghi, Winson Han, Eli VanderBilt, Luca Weihs, Alvaro Herrasti, Matt Deitke,
373 Kiana Ehsani, Daniel Gordon, Yuke Zhu, et al. Ai2-thor: An interactive 3d environment for visual ai.
374 *arXiv preprint arXiv:1712.05474*, 2017.
- 375 [45] Chengshu Li, Ruohan Zhang, Josiah Wong, Cem Gokmen, Sanjana Srivastava, Roberto Martín-Martín,
376 Chen Wang, Gabrael Levine, Michael Lingelbach, Jiankai Sun, Mona Anvari, Minjune Hwang, Manasi
377 Sharma, Arman Aydin, Dhruva Bansal, Samuel Hunter, Kyu-Young Kim, Alan Lou, Caleb R Matthews,
378 Ivan Villa-Renteria, Jerry Huayang Tang, Claire Tang, Fei Xia, Silvio Savarese, Hyowon Gweon, Karen
379 Liu, Jiajun Wu, and Li Fei-Fei. BEHAVIOR-1k: A benchmark for embodied AI with 1,000 everyday
380 activities and realistic simulation. In *6th Annual Conference on Robot Learning*, 2022. URL https://openreview.net/forum?id=_8DoIe8G3t.
- 382 [46] Erwin Coumans and Yunfei Bai. Pybullet, a python module for physics simulation for games, robotics and
383 machine learning. 2016.
- 384 [47] Debidatta Dwibedi, Yusuf Aytar, Jonathan Tompson, Pierre Sermanet, and Andrew Zisserman. Counting
385 out time: Class agnostic video repetition counting in the wild. In *Proceedings of the IEEE/CVF conference*
386 *on computer vision and pattern recognition*, pages 10387–10396, 2020.
- 387 [48] Huazhang Hu, Sixun Dong, Yiqun Zhao, Dongze Lian, Zhengxin Li, and Shenghua Gao. Transrac:
388 Encoding multi-scale temporal correlation with transformers for repetitive action counting. In *Proceedings*
389 *of the IEEE/CVF Conference on Computer Vision and Pattern Recognition*, pages 19013–19022, 2022.
- 390 [49] Yunhua Zhang, Ling Shao, and Cees GM Snoek. Repetitive activity counting by sight and sound. In
391 *Proceedings of the IEEE/CVF conference on computer vision and pattern recognition*, pages 14070–14079,
392 2021.
- 393 [50] Saptarshi Sinha, Alexandros Stergiou, and Dima Damen. Every shot counts: Using exemplars for repetition
394 counting in videos. *arXiv preprint arXiv:2403.18074*, 2024.

395 **Checklist**

- 396 1. For all authors...
- 397 (a) Do the main claims made in the abstract and introduction accurately reflect the paper’s
- 398 contributions and scope? [Yes]
- 399 (b) Did you describe the limitations of your work? [Yes]
- 400 (c) Did you discuss any potential negative societal impacts of your work? [Yes]
- 401 (d) Have you read the ethics review guidelines and ensured that your paper conforms to
- 402 them? [Yes]
- 403 2. If you are including theoretical results...
- 404 (a) Did you state the full set of assumptions of all theoretical results? [N/A]
- 405 (b) Did you include complete proofs of all theoretical results? [N/A]
- 406 3. If you ran experiments (e.g. for benchmarks)...
- 407 (a) Did you include the code, data, and instructions needed to reproduce the main experi-
- 408 mental results (either in the supplemental material or as a URL)? [Yes]
- 409 (b) Did you specify all the training details (e.g., data splits, hyperparameters, how they
- 410 were chosen)? [N/A] We did not do any training.
- 411 (c) Did you report error bars (e.g., with respect to the random seed after running experi-
- 412 ments multiple times)? [No] We do not train any models, and we only run inference
- 413 with existing checkpoints.
- 414 (d) Did you include the total amount of compute and the type of resources used (e.g., type
- 415 of GPUs, internal cluster, or cloud provider)? [Yes]
- 416 4. If you are using existing assets (e.g., code, data, models) or curating/releasing new assets...
- 417 (a) If your work uses existing assets, did you cite the creators? [Yes] We cited OmniGibson
- 418 properly.
- 419 (b) Did you mention the license of the assets? [Yes] OmniGibson is under MIT License.
- 420 (c) Did you include any new assets either in the supplemental material or as a URL? [Yes]
- 421 (d) Did you discuss whether and how consent was obtained from people whose data you’re
- 422 using/curating? [Yes]
- 423 (e) Did you discuss whether the data you are using/curating contains personally identifiable
- 424 information or offensive content? [N/A]
- 425 5. If you used crowdsourcing or conducted research with human subjects...
- 426 (a) Did you include the full text of instructions given to participants and screenshots, if
- 427 applicable? [N/A]
- 428 (b) Did you describe any potential participant risks, with links to Institutional Review
- 429 Board (IRB) approvals, if applicable? [N/A]
- 430 (c) Did you include the estimated hourly wage paid to participants and the total amount
- 431 spent on participant compensation? [N/A]

432 **A Appendix**

433 Due to space limit, we only included the performance of Gemini-1.5-Flash for variations of the
 434 benchmarks in Section 4.3. Below we present the full evaluation results for all models.

Table 4: Overall results for different models on occlusion version.

Model	OBZ	OBO	OBF	MAE	RMSE	CORR
Video-LLaVA	0.02	0.06	0.23	0.87	14.08	0.44
PLLaVA	0.01	0.10	0.30	0.76	12.60	0.46
VideoChat2	0.04	0.12	0.41	1.29	11.63	-0.04
Video-ChatGPT	0.02	0.07	0.30	1.02	12.41	0.08
LLOVi	0.07	0.22	0.52	0.74	8.74	0.51
Gemini-1.5-Flash	0.10	0.21	0.52	0.50	8.48	0.77
Gemini-1.5-Pro	0.06	0.16	0.45	0.55	9.45	0.85

Table 5: Overall results for different models on nonuniform version.

Model	OBZ	OBO	OBF	MAE	RMSE	CORR
Video-LLaVA	0.01	0.06	0.25	0.89	14.34	0.30
PLLaVA	0.01	0.07	0.27	0.79	13.07	0.45
VideoChat2	0.04	0.11	0.43	1.04	9.13	0.19
Video-ChatGPT	0.04	0.09	0.30	1.09	12.38	0.09
LLOVi	0.05	0.16	0.53	0.69	9.06	0.50
Gemini-1.5-Flash	0.09	0.17	0.48	0.51	8.92	0.75
Gemini-1.5-Pro	0.06	0.15	0.45	0.54	9.43	0.81

Table 6: Overall results for different models on 5-second version.

Model	OBZ	OBO	OBF	MAE	RMSE	CORR
Video-LLaVA	0.01	0.08	0.23	0.90	14.24	0.27
PLLaVA	0.01	0.09	0.29	0.79	13.14	0.43
VideoChat2	0.04	0.13	0.42	1.06	9.05	0.19
Video-ChatGPT	0.03	0.10	0.35	0.95	11.76	0.22
LLOVi	0.04	0.11	0.33	0.77	12.29	0.28
Gemini-1.5-Flash	0.04	0.11	0.37	0.65	10.70	0.74
Gemini-1.5-Pro	0.03	0.09	0.33	0.65	11.14	0.82

Table 7: Overall results for different models on 2-minute version.

Model	OBZ	OBO	OBF	MAE	RMSE	CORR
Video-LLaVA	0.01	0.07	0.23	0.86	14.05	0.40
PLLaVA	0.03	0.08	0.27	0.80	13.29	0.44
VideoChat2	0.04	0.11	0.46	1.02	9.76	0.29
Video-ChatGPT	0.02	0.12	0.36	0.96	12.39	0.09
LLOVi	0.06	0.19	0.53	0.73	8.92	0.42
Gemini-1.5-Flash	0.10	0.23	0.59	0.45	7.59	0.75
Gemini-1.5-Pro	0.09	0.18	0.50	0.47	8.52	0.83

Table 8: Overall results for different models on egocentric version.

Model	OBZ	OBO	OBF	MAE	RMSE	CORR
Video-LLaVA	0.03	0.09	0.30	0.71	11.32	0.64
PLLaVA	0.05	0.16	0.48	0.62	9.45	0.49
VideoChat2	0.06	0.14	0.46	1.06	8.32	0.25
Video-ChatGPT	0.03	0.10	0.33	0.99	12.87	0.00
LLOVi	0.06	0.14	0.47	0.98	9.84	0.31
Gemini-1.5-Flash	0.10	0.27	0.64	0.54	6.16	0.70
Gemini-1.5-Pro	0.09	0.22	0.50	0.42	8.52	0.82